Mass and salt transfers and halocline depths in an estuary

By ROBERT R. LONG, *Departments of Earth & Planetary Sciences and Mechanics & Materials Science, The Johns Hopkins University, Baltimore, Maryland 21218, USA*

(Manuscript received June 30, 1975; in final form January 22, 1976)

ABSTRACT

The paper considers fluxes of brackish and ocean water out of and into an estuary as well as the depth of the halocline in the estuary. The discussion ignores the details of the mass distribution and circulations in the main body of the estuary (except for the halocline depth) and concentrates on determining the flow conditions and interface depths in the vicinity of the mouth. The flow there is considered to be frictionless and the pressure hydrostatic, and the first part of the analysis, which assumes strong mixing (and, therefore, a deep halocline) in the estuary, yields the same results as those of Stommel and Farmer for their "overmixed" state. Phenomena in this state are determined by a non-dimensional number Q proportional to the fresh water influx q_f. On the other hand, the problem can also be solved when the mixing is zero. The two extreme cases suggest a dependence on a mixing number M for arbitrary mixing. This permits a complete solution for the ocean water flux, brackish water flux, depth of the interface at the mouth, salinity of the brackish water, depth of the halocline in the main body of the estuary and height above sea level of the free surface in the estuary, all as functions of Q_f and M. An interesting feature of all solutions is the main halocline depth which always becomes large for both weak and strong fresh water fluxes and therefore has a minimum at a value q_{fm} which varies with M. This behavior has been observed in Alberni Inlet in British Columbia and in a laboratory experiment by Welander. Comparison of theory with the Baltic Sea leads to some numerical results and speculations.

1. Introduction

We are concerned here with flow and salinity patterns in an estuary and near the mouth of an estuary. We have in mind a body of water like the Baltic Sea, although the model has variable parameters which permit application to almost any estuary whose mouth has a width small compared to the general horizontal dimensions of the estuary. A comparison is also possible with laboratory experiments designed to produce estuarine circulations.

We have neither the inclination nor the competence to discuss at any length the practical importance of studies of estuarine circulations and mass distributions. The problem of pollution of waters near the surface obviously demands attention, but another problem of strong interest for the Baltic and many fjord-type estuaries of Scandinavia is the stagnation of the deep water (Fonselius, 1962, 1967, 1969; Gade, 1970). This is associated with the blocking effects of the sill and other obstructions to deep water motion in conjunction with the stabilizing effects of the typical density increase with depth in an estuary associated with temperature and salinity variations in the vertical. The water motions are very slow and therefore even exceedingly weak density increases with depth greatly inhibit vertical motions. The water stagnation implies very weak or zero turbulence in the deep waters and little turbulent mixing with the fluid above. This in turn cuts off the supply of oxygen from the aerated surface water, and the deep layers may ultimately become completely exhausted of oxygen. This has been a progressive development in the deep Baltic over the past 75 years. One station in the central Baltic shows an oxygen saturation decrease from 30% to near 0% during this period at a depth of 160 m (Fonselius, 1969). Fonselius has warned that the Baltic deep water may soon become devoid of life.

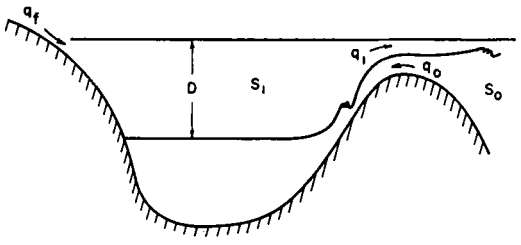

Fig. 1. Model of an estuary.

The complexities of real estuaries have been emphasized by many authors, e.g. Pritchard (1956), Fonselius (1969), Gade (1970) and Welander (1974). The Baltic, for example, is connected to its source of salt water, the Kattegat, by the Danish Belts and the Öresund. This in itself is a great complication compared to our model which is portrayed in part in Fig. 1. The model has a single connection to the ocean. When we compare the model and the Baltic we consider only the Great Belt which, in fact, is mainly responsible for the fluxes into and out of the Baltic. We take the minimum width $\bar{W} = 15$ km for the Great Belt and a mean depth at this section $\bar{h} = 18$ m. In the model, the estuary waters and the flow at the mouth are divided into two layers by a thin interface, described as the halocline in the main portions of the estuary. This is not a bad approximation for the Baltic which has a permanent halocline of thickness 10 m at a depth $D \simeq 60$ m, although there certainly are vertical and horizontal gradients of salinity above and below the halocline. For example, the salinity of the inflowing water in the Store Belt is about 17.5‰ compared to 11‰ in the Baltic deep water although the model ignores this and assumes no mixing as the ocean water pours into the basin. The salinity of the upper layer in the Baltic is about 7‰. The model assumes that the inflowing water is all ocean water; by way of comparison, some of the outflowing Baltic water mixes with the Skagerak water and recirculates back into the Baltic.

The water balance of the Baltic region involves a close equality of precipitation and evaporation so that the fresh water influx q_f is equal to the river runoff which we take to be $q_f = 1.49 \times 10^{10}$ cm³/sec. The outflowing water has a flux q_1 which is about twice the magnitude of q_f (Brogmus, 1952).

Estuarine circulations are usually very small, of order of centimeters per second or less, and this suggests a consideragle importance of friction. This has been confirmed by many investigations (e.g. Pritchard, 1956) and the author has treated this theoretically (Long, 1975*a*). At a narrow mouth, however, speeds increase very considerably, inertial, pressure and gravity forces become comparable (Long, 1975*a*) and friction beomes relatively much less important. In the present paper we confine attention to flows near the mouth and we neglect friction entirely in this region.

As the fresh water enters the estuary, it tends to mix with the salt water from the lower levels. This mixing is caused primarily by turbulence near the halocline (1) arising from local shears imposed by tidal currents and currents due to wind stresses applied to the water surface, or shears associated with the motions of the estuarine circulation, or (2) arising from a flux of turbulent energy from higher levels (energy flux divergence term in the turbulent energy equation), or (3) arising from convection due to local decreases of mean temperature with height. Turbulence in layers below the halocline will be much weaker and is ignored in the model.

We relate the mixing to laboratory experiments designed to study turbulence in a stably stratified liquid. The first of these was by Rouse & Dodu (1955) and consisted of a vessel with two layers of liquid of different densities as in Fig. 2. A grid of metal bars was oscillated vertically in the upper layer with a small stroke a, and observations were made of the *entrainment velocity*, u_e, or downward propagation of the interface. In this and other figures, the interface is shown as a discontinuity of density. Actually it is a thin layer of thickness 1–2 cm. Some experiments (Moore & Long, 1971; Long, 1973) suggest that the interface thickness is proportional to the interface depth

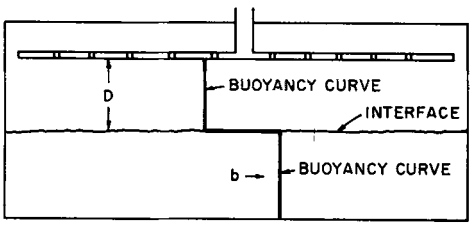

Fig. 2. Mixing experiment of Rouse and Dodu.

D with a constant of proportionality of about 1/6. This agrees well with estimates in the Baltic cited above.

A number of investigators have studied experiments similar to that in Fig. 2 (Cromwell, 1960; Turner, 1968; Brush, 1970; Wolanski, 1972; Turner, 1973; Linden, 1973; Crapper, 1973; Crapper & Linden, 1974; and unpublished observations by Claes Rooth). It is possible, for example, to obtain a statistically steady state by supplying fluid to the lower layer and by adding and subtracting fluid from the upper layer. This has an obvious analogy to an estuary with the influx of ocean water in the lower layer, and the influx of fresh water and the outflow of brackish water in the upper layer.

In these stirring experiments at large Reynolds and Péclet numbers (Crapper & Linden, 1974), it appears that the entrainment velocity obeys a relationship

$$\frac{u_e}{u_*} = K_n Ri_*^{-3/2}, \quad Ri_* = \frac{D\Delta b}{u_*^2} \tag{1}$$

where D is the depth of the mixed layer, and $u_* = \omega a$, where ω is the frequency of oscillation of the grid. K_n is a constant and Δb is the increment of buoyancy across the interface. Buoyancy is defined by

$$b = \frac{(\varrho - \varrho_f)}{\varrho_f} g$$

where ϱ is density, ϱ_f is the density of fresh water and g is gravity.

Several experiments have been constructed to introduce shearing currents in turbulent density-stratified systems in an effort to simulate atmospheric and oceanic phenomena. The first of these of direct relevance to our discussion was that of Kato & Phillips (1969). The apparatus was a large circular annular channel filled with salt water with an initial linear density gradient. A constant stress $\tau = u_*^2$ was applied by rotating a flat screen at the surface (Fig. 3). They found, for larger values of Ri_*,

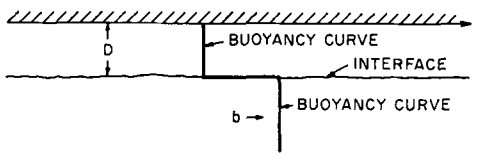

Fig. 3. Experiment of Kato and Phillips.

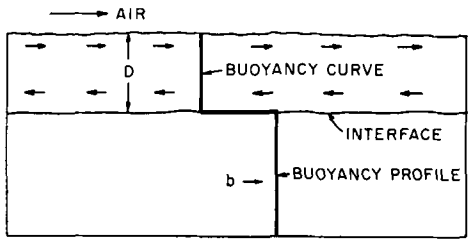

Fig. 4. Wu's experiment.

$$\frac{u_e}{u_*} = K_s Ri_*^{-1} \tag{2}$$

where Ri_* is of the same form as in eq. (1) although u_* has a different meaning. The same experiment with a lower layer of uniform density is now being investigated by Prof. Phillips and L. Kantha at The Johns Hopkins University.

Also of interest is a recent experiment by Wu (1973), shown schematically in Fig. 4, in which the source of the shear was a current of air blowing over a vessel containing a two-fluid system. Wu also obtained eq. (2).

The experiments with and without shear appear to be governed by different laws, but the author (Long, 1975*b*) has offered a unified theory which may be expressed as

$$\frac{u_e}{\sigma_u} = K' Ri^{-1}, \quad Ri = \frac{l\Delta b}{\sigma_u^2} \tag{3}$$

where σ_u is the rms horizontal turbulent velocity near the interface and l is the integral length scale. It is reasonable to assume that l is proportional to the depth of the mixed layer and we therefore adopt the form

$$\frac{u_e}{\sigma_u} = K_* \frac{\sigma_u^2}{D\Delta b} \tag{4}$$

where we estimate $K_* \cong 0.093$ from experiments (Long, 1975*a*). Eq. (4) is used in the discussion of the halocline depth in an estuary in the sections below and we avoid, thereby, the need to introduce eddy-diffusion coefficients.

It is instructive to compute the entrainment velocity for two choices of the quantities in

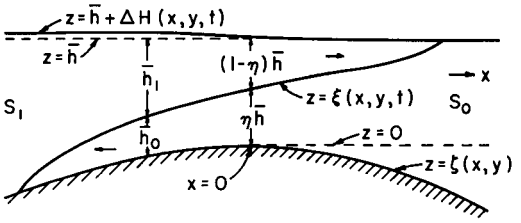

Fig. 5. Conditions near the mouth in a vertical section.

eq. (4). In the Baltic, for example, if we use the salinity difference of 4‰, we get $\Delta b \cong 3.2$ cm/sec². The turbulent intensity is very uncertain and u_e is sensitive to its value, but if we use an estimate $\sigma_u = 1.4$ cm/sec suggested by a discussion near the end of Section 4, and $D = 60$ m, we get $u_e = 1.1$ cm/day. This suggests very slow adjustments to changes in fresh water supply and turbulent intensities. In estuaries in which tidal effects are large σ_u may be much larger. If we use $\sigma_u = 10$ cm/sec, $D = 15$ m, $\Delta b = 10$ cm/sec², more appropriate, say, to estuaries in British Columbia (Pickard & Rodgers, 1959), we obtain $u_e = 5$ m/day and adjustments to changes will be very rapid.

2. Analysis of flows and interface depths near the mouth for deep halocline

Fig. 5 is a picture of conditions near the mouth. The plane $z = 0$ is taken at the average level of the bottom of the channel at the control section, and $\bar{h}$ is the height of the free surface of the open ocean. Elsewhere the free surface has a height $\bar{h} + \Delta H(x, y, t)$ where ΔH is very small and negligible in the analysis except where it contributes to horizontal pressure gradients. In the main body of the estuary (as $x \to -\infty$), $\Delta H = \Delta H_0$ where ΔH_0 is constant. The equation of the interface is $z = \xi(x, y, t)$ and we picture it in Fig. 5 after the initial instant at which time we assume that both fluids were at rest, separated by a partition at the control section with a free surface elevation $\bar{h}$ for $x \geqslant 0$ and $\bar{h} + \Delta H_0$ for $x \leqslant 0$. In the actual estuary the elevation ΔH_0 is directly related to the fresh water influx q_f and, perhaps, to some measure of the mixing, but these relationships may be ignored in the analysis of conditions near the mouth. Fig. 6 shows a horizontal section with width B and a minimum width W. Averages of these vertically are denoted by $\overline{B}$ and $\overline{W}$.

Let us now write down a complete statement of the initial-value problem. We will neglect friction and diffusion and use the Boussinesq and hydrostatic approximations and the assumption that ΔH is small. The last three assume

$$\frac{\Delta\varrho}{\varrho_f} < 1, \quad \frac{\bar{h}^2}{\lambda^2} < 1, \quad \frac{\Delta H_0}{\bar{h}} < 1 \tag{5}$$

where $\Delta\varrho$ is the density difference between the two fluids and λ is the longitudinal length scale, say a typical radius of curvature for the bottom profile in a plane $y =$ constant for a smoothed bottom topography. Using $\zeta(x, y)$ as the height of the bottom above $z = 0$, the problem is determined by

$$\frac{\partial u_1}{\partial t} + u_1\frac{\partial u_1}{\partial x} + v_1\frac{\partial u_1}{\partial y} = -g\frac{\partial(\Delta H)}{\partial x} \tag{6}$$

$$\frac{\partial v_1}{\partial t} + u_1\frac{\partial v_1}{\partial x} + v_1\frac{\partial v_1}{\partial y} = -g\frac{\partial(\Delta H)}{\partial y} \tag{7}$$

$$\frac{\partial h_1}{\partial t} + \frac{\partial(u_1 h_1)}{\partial x} + \frac{\partial(v_1 h_1)}{\partial y} = 0 \tag{8}$$

$$\frac{\partial u_0}{\partial t} + u_0\frac{\partial u_0}{\partial x} + v_0\frac{\partial u_0}{\partial y} = -g\frac{\partial(\Delta H)}{\partial x} + \Delta b\frac{\partial h_1}{\partial x} \tag{9}$$

$$\frac{\partial v_0}{\partial t} + u_0\frac{\partial v_0}{\partial x} + v_0\frac{\partial v_0}{\partial y} = -g\frac{\partial(\Delta H)}{\partial y} + \Delta b\frac{\partial h_1}{\partial y} \tag{10}$$

$$\frac{\partial h_1}{\partial t} + \frac{\partial(u_0\zeta)}{\partial x} + \frac{\partial(v_0\zeta)}{\partial y} + \frac{\partial(u_0 h_1)}{\partial x} + \frac{\partial(v_0 h_1)}{\partial y} = \bar{h}\left(\frac{\partial u_0}{\partial x} + \frac{\partial v_0}{\partial y}\right) \tag{11}$$

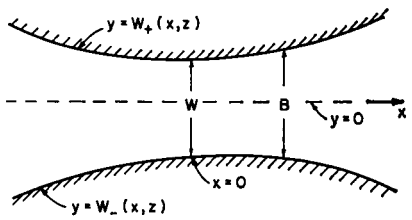

Fig. 6. Conditions near the mouth in a horizontal section.

$$\text{At } x = \infty,\ u_0 = v_0 = u_1 = v_1 = 0,\ \Delta H = 0$$

$$\text{At } x = -\infty,\ u_0 = v_0 = u_1 = v_1 = 0,\ \Delta H = \Delta H_0 \tag{12}$$

$$\text{At } t = 0 \begin{cases} u_0 = v_0 = u_1 = v_1 = 0 \\ \Delta H = \Delta H_0,\ x \leqslant 0; \quad \Delta H = 0, \quad x \geqslant 0 \end{cases}$$

Interface has equation $x = 0$ (13)

In the equations above, u_0, v_0, u_1, v_1 are independent of z. This follows from the hydrostatic assumption and the assumption that the fluids in the main body of the estuary and the open ocean are at rest. The latter is a good approximation if speeds in the vicinity of the mouth are considerably larger than in the ocean and the estuary.

Let us now introduce non-dimensional quantities as follows:[1]

$$u_1 = (\Delta b \bar{h})^{1/2} u_1', \quad v_1 = (\Delta b \bar{h})^{1/2} \frac{\overline{W}}{\lambda} v_1',$$

$$u_0 = (\Delta b \bar{h})^{1/2} u_0', \quad v_0 = (\Delta b \bar{h})^{1/2} \frac{\overline{W}}{\lambda} v_0'$$

$$\zeta = \bar{h}\zeta', \quad h_1 = \bar{h} h_1', \quad \Delta H = \Delta H_0 \Delta H', \quad x = \lambda x',$$

$$y = \overline{W} y' \quad t = \frac{\lambda t'}{(\Delta b \bar{h})^{1/2}} \tag{14}$$

Eqs. (6)–(13) become

$$\frac{\partial u_1'}{\partial t'} + u_1' \frac{\partial u_1'}{\partial x'} = -\beta \frac{\partial (\Delta H')}{\partial x'} \tag{15}$$

$$0 = -\beta \frac{\partial (\Delta H')}{\partial y'} \tag{16}$$

$$\frac{\partial h_1'}{\partial t'} + \frac{\partial (u_1' h_1')}{\partial x'} + \frac{\partial (v_1' h_1')}{\partial y'} = 0 \tag{17}$$

$$\frac{\partial u_0'}{\partial t'} + u_0' \frac{\partial u_0'}{\partial x'} = -\beta \frac{\partial (\Delta H')}{\partial x'} + \frac{\partial h_1'}{\partial x'} \tag{18}$$

$$0 = -\beta \frac{\partial (\Delta H')}{\partial y'} + \frac{\partial h_1'}{\partial y'} \tag{19}$$

[1] Although $\overline{W}$ does not occur explicity in eqs. (6)–(13), it occurs implicitly in the expression for $\zeta(x, y)$.

$$\frac{\partial h_1'}{\partial t'} + \frac{\partial (u_0' \zeta')}{\partial x'} + \frac{\partial (v_0' \zeta')}{\partial y'} + \frac{\partial (u_0' h_1')}{\partial x'} + \frac{\partial (v_0' h_1')}{\partial y'} = \frac{\partial u_0'}{\partial x'} + \frac{\partial v_0'}{\partial y'} \tag{20}$$

$$\text{At } x' = \infty, \quad u_0' = v_0' = u_1' = v_1' = 0, \quad \Delta H' = 0$$

$$\text{At } x' = -\infty, \quad u_0' = v_0' = u_1' = v_1' = 0, \quad \Delta H' = 1 \tag{21}$$

$$\text{At } t' = 0 \begin{cases} u_0' = v_0' = u_1' = v_1' = 0 \\ \Delta H' = 1, \quad x' \leqslant 0; \quad \Delta H' = 0, \quad x' \geqslant 0 \end{cases}$$

Interface has equation $x' = 0$ (22)

where

$$\beta = \frac{\Delta H_0}{\bar{h} \Delta \varrho / \varrho_f} \tag{23}$$

and where we have assumed, in addition to eq. (5),

$$\frac{\overline{W}^2}{\lambda^2} \ll 1, \quad \frac{\overline{W}^2}{\lambda^2} \ll \beta \tag{24}$$

Because of eq. (24), ΔH, and the depth of the interface depend only on x and t. Notice also that eq. (24) and the assumption of irrotationality permit the neglect of $\partial u_0'/\partial y'$ and $\partial u_1'/\partial y'$ in eqs. (15) and (18). Notice also that we have neglected any influence of the depth of the halocline in the estuary. If the depth is D, we are, in effect, now assuming

$$\frac{\bar{h}}{D} \ll 1 \tag{25}$$

As a result of the approximations in eq. (5), (24) and (25), the flow depends on only one non-dimensional number β. We will see that β is of order one (actually 1/2) even when $\Delta H_0 \to 0$.

After some time, conditions near the mouth will become steady and, reverting to dimensional notation, we obtain the two approximate Bernoulli equations

$$\frac{u_1^2}{2} + g \Delta H = g \Delta H_0 \tag{26}$$

$$\frac{u_0^2}{2} + g \Delta H - \Delta b h_1 = 0 \tag{27}$$

where we have assumed the behavior $h_1 \to 0$ as $x \to \infty$. Eliminating $g\Delta H$ and introducing the constant fluxes q_0 and q_1, we obtain

$$\frac{q_0^2}{2\bar{h}_0^2 \bar{B}^2 \Delta b} - \frac{q_1^2}{2h_1^2 \bar{B}^2 \Delta b} - h_1 + \beta\bar{h} = 0 \tag{28}$$

where we ignore the difference in mean channel width in the two layers. The quantity $\bar{h}_0$ is the depth of the lower fluid averaged over a section. Differentiating eq. (28), we obtain

$$\frac{dh_1}{dx}(F_0^2 + F_1^2 - 1) = -F_0^2 \frac{d\xi}{dx} + 2(h_1 - \beta\bar{h}) \frac{1}{\bar{B}} \frac{d\bar{B}}{dx} \tag{29}$$

where the Froude numbers are defined by

$$F_0^2 = \frac{q_0^2}{\bar{h}_0^3 \bar{B}^2 \Delta b}, \qquad F_1^2 = \frac{q_1^2}{h_1^3 \bar{B}^2 \Delta b}$$

where ξ is the elevation of the bottom above $z = 0$ averaged across the section. At the control section, by definition, the water depth is constant or a minimum and the channel width is a minimum, so that the rhs of eq. (29) is zero there. Let us assume, tentatively, $dh_1/dx = 0$ at the control section. Differentiating eq. (29) again, we obtain an additional equation at the control section,

$$0 = -F_0^2 \frac{d^2\xi}{dx^2} + 2(h_1 - \beta\bar{h}) \frac{1}{\bar{B}} \frac{d^2\bar{B}}{dx^2} \tag{30}$$

where we have put $d^2h_1/dx^2 = 0$ because, on physical grounds, h_1 should be neither a maximum nor a minimum at the control section.[1] Eq. (30) is highly unlikely because we would not anticipate that the velocities and the interface depth are sensitively dependent on boundary curvatures. We conclude that $dh_1/dx \neq 0$ at the control section and that

$$F_0^2 + F_1^2 = 1 \tag{31}$$

Eq. (31) is the critical conditions of Stommel & Farmer (1952, 1953) and we adopt it here.

If we combine eqs. (28) and (31), and denote by $\eta\bar{h}$ the height of the interface above $z = 0$, we obtain

$$F_1^2 = 3\eta - 2 + 2\beta \tag{32}$$

$$F_0^2 = 3 - 3\eta - 2\beta \tag{33}$$

In view of eqs. (15)–(22), F_1^2, F_0^2 and η are all functions of β only.

Let us now investigate the form of eqs. (15)–(22) in a somewhat simpler geometry in which the bottom is level near the mouth, the channel widens indefinitely for $|x| = \infty$ and the width is symmetrical about $x = 0$. We use the transformations

$$\beta\Delta H'(x', t') - h_1'(x', t') = \beta\Delta H^*(x^*, t^*) - \beta$$

$$h_1'(x', t') = -h_1^*(x^*, t^*) + 1$$

$$u_0'(x', y', t') = -u_1^*(x^*, y^*, t^*),$$

$$v_0'(x', y', t') = v_1^*(x^*, y^*, t^*)$$

$$u_1'(x', y', t') = -u_0^*(x^*, y^*, t^*),$$

$$v_1'(x', y', t') = v_0^*(x^*, y^*, t^*)$$

$$x' = -x^*, \quad y' = y^*, \quad t' = t^* \tag{34}$$

In terms of these starred variables, the equations and boundary and initial conditions are identical to those in eqs. (15)–(22) (after setting $\zeta' = 0$) *provided* $\beta = \beta_0 = \frac{1}{2}$, and the invariance may be used to show that $\eta = \frac{1}{2}$. Obviously this corresponds to small q_f and using eqs. (32) and (33) we may write

$$F_1^2 = F_0^2 = \tfrac{1}{2}, \quad \eta = \tfrac{1}{2}, \quad \beta = \tfrac{1}{2} \quad \text{for small } q_f \tag{35}$$

Although the model is somewhat simplified, we assume that (35) holds in the general case.

On the other hand, let q_f increase to a value q_{fc} at which η just becomes zero. We picture the situation in Fig. 7. To the right of the interface the velocities are zero, and differentiating eq. (28) in the region $x \geq 0$, we get at the control section

$$(F_1^2 - 1) \frac{dh_1}{dx} = 0$$

[1] The situation is different from water flow over an obstacle in a stream in which the slope of the free surface can be zero at the obstacle crest. In the present case the light brackish fluid spreads laterally as it enters the ocean and the interface should rise sharply. The heavy ocean water moving into the estuary also contributes to a strong slope of the interface.

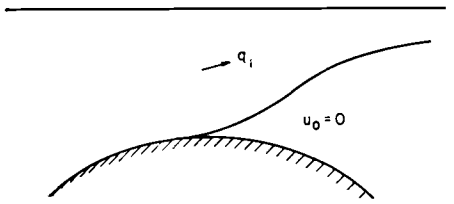

Fig. 7. Conditions near the mouth when basin fills with fresh water.

Thus

$$F_1^2 = 1, \quad F_0^2 = 0, \quad \eta = 0, \quad \beta = \tfrac{3}{2} \quad \text{for } q_{fc} \tag{36}$$

We will now assume simple linear forms for F_1^2 and F_0^2 as functions of β (or η) satisfying the extremes in eqs. (35) and (36), namely,

$$F_1^2 = 1 - \eta, \quad F_0^2 = \eta, \quad \beta = \tfrac{3}{2}(1 - \tfrac{4}{3}\eta) \tag{37}$$

There are several consequences of the assumption in eq. (37). If we differentiate eq. (29), at the control section, we obtain

$$3\left(\frac{dh_1}{dx}\right)^2 \left(\frac{F_0^2}{\eta} - \frac{F_1^2}{1-\eta}\right) = -F_0^2 \bar{h} \frac{d^2\zeta}{dx^2} + 2\bar{h}^2(1-\eta-\beta)\frac{1}{\bar{B}}\frac{d^2\bar{B}}{dx^2} \tag{38}$$

We see from eq. (37) that the left-hand side of (38) vanishes whereas the right hand side is non-zero of order h^2/λ^2. In view of the approximations made in the development, we conclude that a consequence of eq. (37) is that the slope of the interface at the control section is much larger[1] than h/λ. It follows from eqs. (35), (36) and (38) that the interface slope is large when q_f is small and large, and the likelihood that it is true for other fluxes establishes the plausibility of the assumed forms in eq. (37).

The equations for the Froude numbers in eq. (37) are identical to those found by Stommel & Farmer (1952, 1953) and we should discuss the relationship of their approach to that of the present paper. They argued that for weak mixing the fresh water should flow directly to the mouth in a layer of finite thickness over a stagnant body of ocean water. As mixing increases, the salinity S_1 of the outflowing water increases. If we combine the critical condition and mass and salt conservation, we may write

$$\frac{Q_f^2(1-\Delta S)^2}{\eta^3} + \frac{Q_f^2}{(1-\eta)^3} = (\Delta S)^3, \quad Q_f^2 = \frac{q_f^2}{b_0 \bar{h}^3 \overline{W}^2} \tag{39}$$

where $\Delta S = (S_0 - S_1)/S_0$ and S_0 is the salinity and b_0 the buoyancy of ocean water. If at a given Q_f, ΔS is a minimum for variations of η, i.e., if

$$\frac{d(\Delta S)}{d\eta} = 0 \tag{40}$$

we obtain

$$(1 - \Delta S) = \frac{\eta^2}{(1-\eta)^2} \tag{41}$$

and this is easily seen to be equivalent to the results in eq. (37). This extreme state was called "overmixed" by Stommel & Farmer.

Let us now attempt to establish this result in terms of the approach in this section. In the general case of arbitrary mixing the problem is determined by two parameters Q_f and a parameter involving the turbulent intensity. We will define this parameter in the next section as

$$M = \frac{b_0^{3/2} \bar{h}^{5/2} \overline{W}}{A K_* \sigma_u^3} \tag{42}$$

where A is the area of the estuary and K_* and σ_u appear in eq. (4). When the mixing is zero, M is infinite. We may presume that the "overmixed" state corresponds to $M = 0$. In our present version of the problem, we find[2] that $D \to \infty$ as $M \to 0$, and therefore variations in ΔS become insensible as $M \to 0$, i.e.,

$$\frac{d(\Delta S)}{dD} = \frac{d(\Delta S)}{dM}\frac{dM}{dD} \to 0 \quad \text{as} \quad M \to 0 \tag{43}$$

where we keep Q_f fixed. Since η is a function of M, we may also write

$$\frac{d(\Delta S)}{d\eta}\frac{d\eta}{dM}\frac{dM}{dD} \to 0 \quad \text{as} \quad M \to 0 \tag{44}$$

[1] Since the interface slope is much greater than the bottom slope, we justify *a posteriori* the neglect of the bottom slope in deriving (35).

[2] This follows below from eq. (46).

If it were possible to establish that $d\eta/dM$ and dM/dD are finite and different from zero as $M \to 0$, then Stommel & Farmer's assumption, $d(\Delta S)/d\eta = 0$, would follow from the more physical assumption in (43). The author has been unsuccessful in establishing this behavior of $d\eta/dM$ and dM/dD; indeed in the determination of the problem in the next section, all three derivatives in eq. (44) tend to zero as $M \to 0$. The condition $d(\Delta S)/d\eta = 0$ and the Stommel & Farmer theory seem well established on the basis of the close agreement with laboratory experiment and we will accept eq. (37) for $M \to 0$ in the next section.

3. Solution for arbitrary mixing and fresh-water influx

We have the behavior of eq. (37) as one extreme:

$$F_1^2 = (1-\eta), \quad F_0^2 = \eta, \quad \beta = \frac{3}{2}\left(1 - \frac{4}{3}\eta\right) \quad \text{as} \quad M \to 0 \tag{45}$$

When the mixing is finite, $\bar{h}/D$ is no longer small and we have the additional eq. (4) which may be written

$$q_0 = \frac{AK_* \sigma_u^3}{D\Delta b} \tag{46}$$

or

$$Q_f(1-\Delta S) = \frac{1}{D_* M}, \quad D_* = \frac{D}{\bar{h}}, \quad M = \frac{b_0^{3/2}\bar{h}^{5/2}\overline{W}}{AK_*\sigma_u^3} \tag{47}$$

Let us consider the opposite extreme of $\sigma_u \to 0$. Then $M \to \infty$, $q_0 \to 0$, $F_0^2 \to 0$, $F_1^2 \to 1$ and eq. (32) yields

$$F_1^2 = 1, \quad F_0^2 = 0, \quad \beta = \tfrac{3}{2}(1-\eta) \quad \text{as} \quad M \to \infty \tag{48}$$

If we now compare the expression for β for the two extremes corresponding to $M = 0$ and $M = \infty$, we may attempt to construct an expression for β as a function of η and M for the general case. A simple form which satisfies the two extremes, $\beta \to \frac{3}{2}(1-\eta)$ as $M \to \infty$ and $\beta = \frac{3}{2}(1 - \frac{4}{3}\eta)$ as $M \to 0$ is

$$\beta = \frac{3}{2}\left[1 - \frac{\eta[4 + 3(\alpha M)^s]}{3[1 + (\alpha M)^s]}\right] \tag{49}$$

where α and s are constants. There are additional requirements which must be satisfied, however. Thus as $\sigma_u \to 0$ it follows from eqs. (27) and (48) that

$$\frac{\Delta H_0}{h_1 \Delta\varrho/\varrho_f} \to \frac{3}{2}, \quad \frac{\Delta H_0}{D\Delta\varrho/\varrho_f} \to 1 \tag{50}$$

The result $D/h_1 = \frac{3}{2}$ has been derived by Binney (1972). Eq. (47) indicates

$$(1-\Delta S) \to \frac{K_* A \sigma_u^3}{(3/2) q_f b_0 h_1}$$

A combination of eq. (33) and eq. (49) yields

$$\frac{q_0^2}{h_0^3 \Delta b \overline{W}^2} = \frac{\eta}{1 + (\alpha M)^s}$$

According to eq. (46)

$$\frac{A^2 K_*^2 \sigma_u^6}{D^2 (\Delta b)^3 h_0^3 \overline{W}^2} = \frac{h_0}{\bar{h}}\left[1 + \alpha^s\left(\frac{b_0^{3/2}\bar{h}^{5/2}\overline{W}}{AK_*\sigma_u^3}\right)^s\right]^{-1} \tag{51}$$

As $\sigma_u \to 0$, all other quantities remain finite and we see that $s = 2$. Now consider $\bar{h} \to \infty$, $h_0 \to \infty$. Then $M \to \infty$. Since all other quantities remain finite, eq. (51) cannot be satisfied. We may overcome this by replacing $(\alpha M)^2$ by $(\alpha M)^2(1-\eta)^2$ and the two extreme forms for β are still satisfied. We now notice that eq. (51) should be correct as $\sigma_u \to 0$ no matter what the depth h_0 is because the lower fluid comes to rest. This is not possible, however, and accordingly we replace $(\alpha M)^2(1-\eta)^2$ by $(\alpha M)^2(1-\eta)^2\eta^4$. Since $D \to \frac{3}{2}h_1$, $\Delta b \to b_0$, as $\sigma_u \to 0$, eq. (51) yields $\alpha = \frac{3}{2}$. With these choices, the problem is now determined by the equations

$$\beta = \frac{3}{2}\left[1 - \frac{\eta[16 + 27M^2(1-\eta)^2\eta^4]}{3[4 + 9M^2(1-\eta)^2\eta^4]}\right] \tag{52}$$

$$Q_f^2 = \frac{(\Delta S)^3(1-\eta)^3[4 + 9M^2(1-\eta)^2\eta^4 - 4\eta]}{[4 + 9M^2(1-\eta)^2\eta^4]} \tag{53}$$

$$(1-\Delta S)^2 = \frac{4\eta^4}{(1-\eta)^3[4 + 9M^2(1-\eta)^2\eta^4 - 4\eta]} \tag{54}$$

$$D_* = \frac{1}{Q_f M(1-\Delta S)} \tag{55}$$

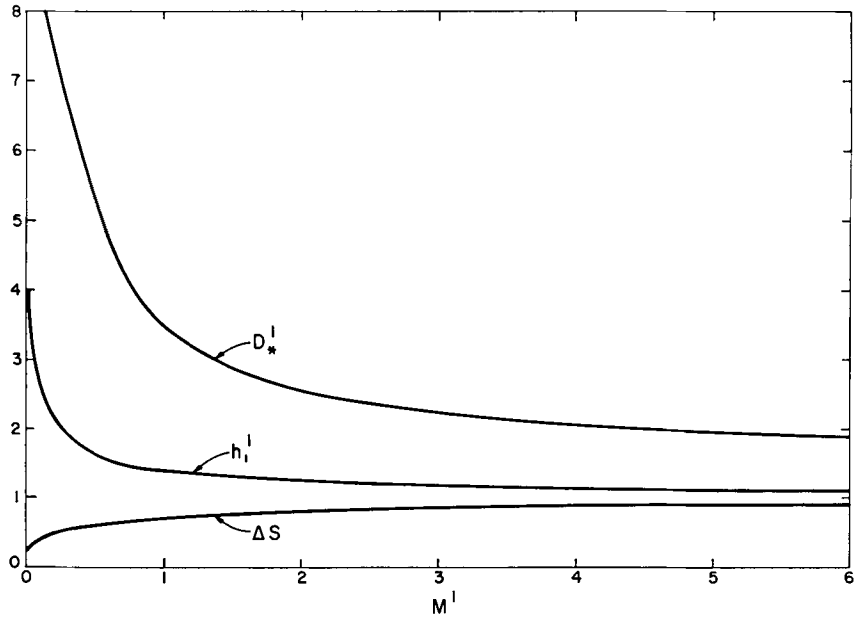

Fig. 8. Interface and halocline depths and salinity differences for an infinitely deep estuary. D'_* and h'_1 are defined in eq. (57).

4. Discussion and numerical results

The simplest example of a solution of eqs. (52)–(55) is an estuary with an infinitely deep sill, i.e., $\hat{h} \to \infty$. The solution then depends on a single non-dimensional number

$$M' = \frac{q_f^{5/3} b_0^{2/3}}{A K_* \sigma_u^3 \overline{W}^{2/3}} \tag{56}$$

Using the definitions

$$D'_* = \frac{D b_0^{1/3} \overline{W}^{2/3}}{q_f^{2/3}}, \quad h'_1 = \frac{h_1 b_0^{1/3} \overline{W}^{2/3}}{q_f^{2/3}} \tag{57}$$

We get

$$D'_* = \frac{1}{M'(1-\Delta S)}, \quad h'_1 \Delta S = 1,$$

$$(1-\Delta S) = \frac{2}{3M' h'^{5/2}} \tag{58}$$

Results are shown in Fig. 8. The depth of the interface at the mouth h_1 and the halocline depth D increase monotonically as M' decreases (mixing increases). D is about twice as large as h_1 for larger M' over most of the range of M'. The salinity of the outflowing fluid increases monotonically as the mixing increases and the fresh water flux decreases. The flux of the outflowing fluid changes very slowly with M' over most of the range, $q_1/q_f = 1/\Delta S$ increasing from 1.0 to 1.5 as M decreases from infinity to $M' \cong 1$. Below $M' = 1$, q_1/q_f increases more rapidly but only begins to exceed 2.0 when M' drops below $M' = 0.1$.

When the sill depth is finite, eqs. (52)–(55) reveal a common behavior for all values of M, namely that the halocline is very deep for both small and large values of the fresh-water flux q_f, with a minimum at a value of Q_{fm} determined by M. The quantity Q_{fm} decreases with M; for example $Q_{fm} = 0.244$ at small M, $Q_{fm} = 0.08$ at $M = 100$ and $Q_{fm} = 0.03$ at $M = 1\,000$. The behavior of D_* as a function of Q_f is shown in Figs. 9 and 10 for smaller and larger values of M, respectively. When M exceeds 100 or so there is little change in the behavior over most of the range of Q_f except near Q_{fm}. There the halocline depth continues to decrease strongly as M gets still larger.

Fig. 11 shows an experiment by Welander (1974) similar to the model of this paper. Data are lacking to permit a careful comparison but $M = 8$ seems a good choice. Constants were

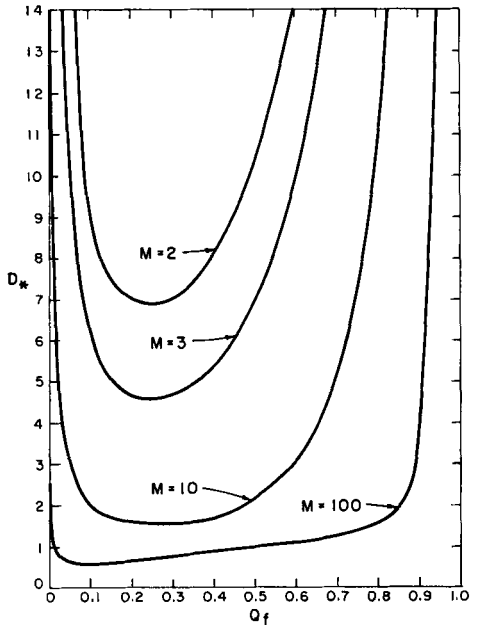

Fig. 9. Halocline depth as function of fresh-water influx for smaller values of M.

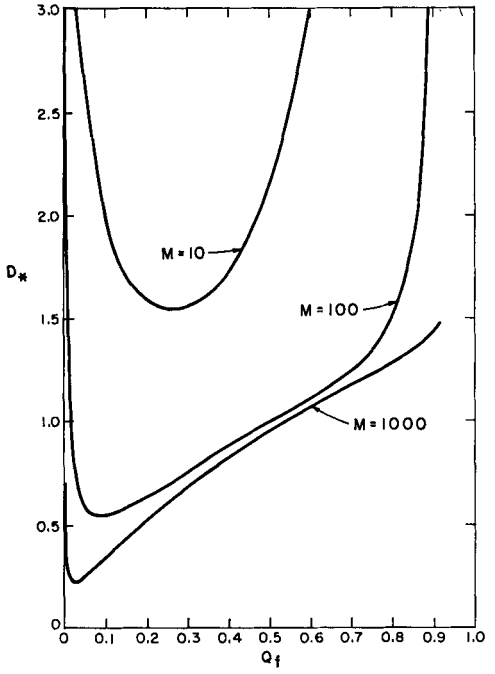

Fig. 10. Halocline depths as function of fresh-water influx for larger values of M.

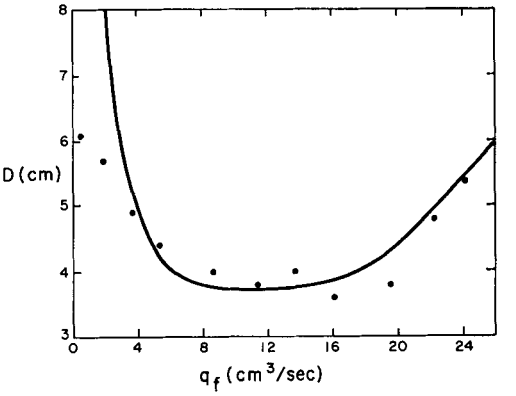

Fig. 11. Halocline depths in Welander's experiment.

chosen to force agreement near the minimum point. The agreement is quite good except for small values of q_f where entrainment velocities are very small and the experiments may not have been in a steady state. An additional factor is the decrease of σ_u near the interface as D increases and the interface gets further and further away from the source of energy (stirrers). This effect is not included in the theory and would tend to reduce D. The tendency for

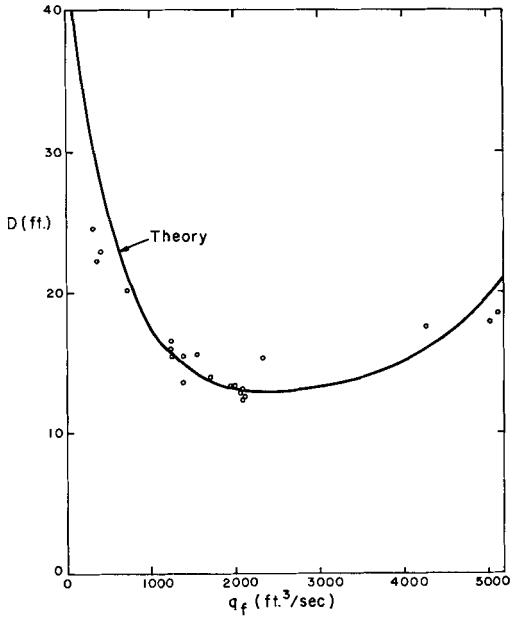

Fig. 12. Observations of halocline depths in Alberni Inlet.

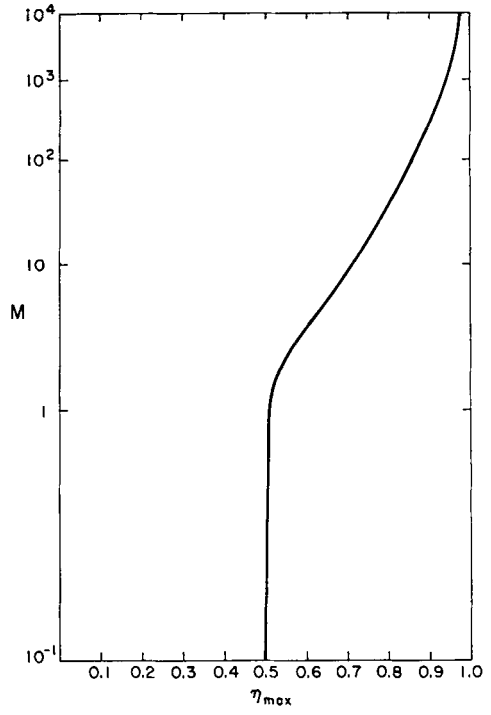

Fig. 13. η_{max} as a function of M.

a minimum depth of the halocline has been observed by Tully (1949) in Alberni Inlet as we see in Fig. 12. The theoretical curve corresponds to $M = 0$.

We have seen that η has a maximum value of 1/2 in the case $M = 0$ when the fresh water influx decreases to zero. The computations reveal that η_{max} increases with M, as we see in Fig. 13, tending to $\eta_{max} = 1$ at very large M.

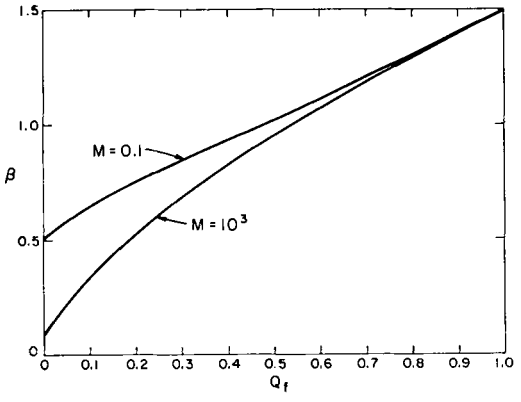

Fig. 14. Variations of β with Q and M.

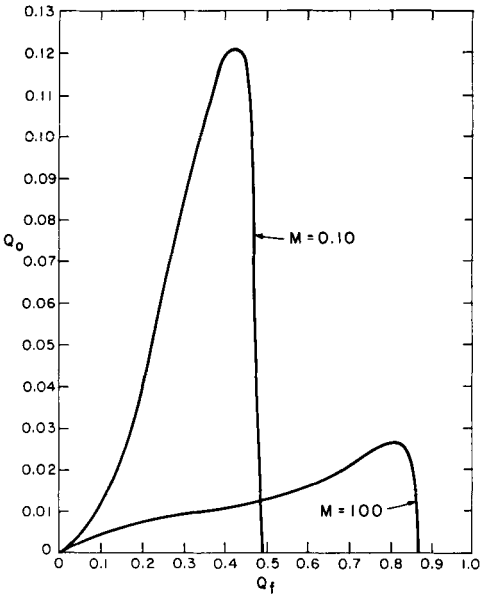

Fig. 15. Variations of ocean water flux with fresh water influx.

The quantity β varies with Q_f and M as seen in Fig. 14. It is interesting to note that $\beta\Delta S \propto \Delta H_0/\bar{h}$ varies very little with M. Indeed, one would anticipate that this quantity would vary more sensitively with Q_f.

The influx of ocean water is negligible for $M > 100$ or so. As mixing increases, Q_0, defined by

$$Q_0 = \frac{q_0}{b_0^{1/2}\bar{h}^{3/2}W}$$

increases. Q_0 rises with increase of Q_f, reaches a maximum and then decreases. Examples are shown in Fig. 15. The curves for $M < 3$ or so do not differ very much from the curve shown for $M = 0.10$. This typical behavior of Q_0 appears in other theories of estuaries, for example Kullenberg (1955).

The salinity of the outflowing fluid increases as the fresh water influx decreases. This was also pointed out by Kullenberg. Fig. 16 shows the curves for two values of M. Decreases in mixing intensities accompany decreases in salinity, as expected.

An estimation of M for various applications is important but M is extremely sensitive to σ_u and σ_u is difficult to estimate. We may make the following computations for the Baltic Sea:

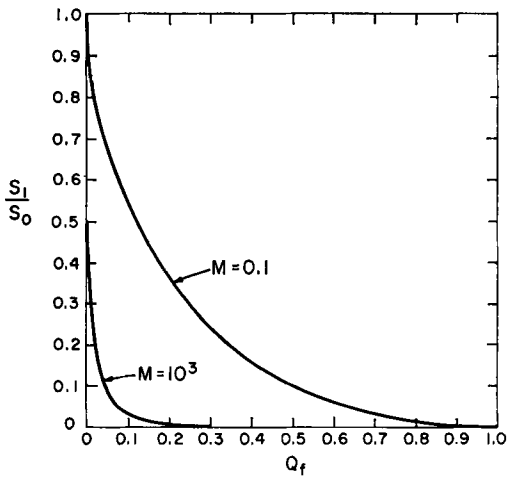

Fig. 16. Salinity of brackish water as a function of fresh water influx.

Fonselius (1969) gives the ratio $q_1/q_f \cong 2$. We may compute Q_f from eq. (28) using the data of Fonselius of $q_f = 1.49 \times 10^{10}$ cm³/sec and width $\overline{W} = 15$ km, depth $\bar{h} = 18$ m for the Great Belt. The appropriate value of b_0 corresponds to a salinity in the lower layer of 17.5‰ or $b_0 = 14$ cm/sec². This leads to $Q_f = 0.0348$. Finally $D/\bar{h}$ for the Baltic is 60/18 or 3.33. If we use the last two figures, we obtain close agreement for a value of $M = 12$. The computations yield $Q_f = 0.0346$ and $D/\bar{h} = 3.45$. The value of q_1/q_f, however, is 3.29 which is considerably too large. The value of $M = 12$ permits us to compute σ_u using $A = 3.1 \times 10^{15}$ cm². We obtain $\sigma_u = 1.4$ cm/sec which is, perhaps, reasonable.

One may speculate regarding the changes in the Baltic over the past 75 years as described by Fonselius. The stability of the Baltic has apparently increased, because, although the salinity of the upper and lower layers have both increased, the salinity of the lower layer has increased somewhat more. This stability increase may be related to the reduction of oxygen in the deep Baltic. q_f has decreased about 15% over this period and Fonselius ascribes the increase of salinity in the Baltic as a whole to this decrease of q_f. A further change has been a decrease in the depth of the halocline from 80 m to 60 m over the period. According to present theory, for the value of $M = 12$ and the other conditions of the Baltic, a decrease of q_f with all other factors held constant should have resulted in an *increase* of D. However, as we have seen, D is most sensitive to σ_u. Since precipitation and runoff have decreased, this implies a decrease of storminess over the Baltic as asserted, in fact, by Fonselius, and a decrease of σ_u. This could have been overriding and serves to explain the decrease of D. Notice that only long period changes in σ_u are involved because we have decided that the response of the halocline depth to changes is very slow.

Acknowledgement

This research was supported by the Office of Naval Research, Fluid Dynamics Division, under Contract No. N00014-75-C-0805, Code N66019.

REFERENCES

Binney, A. M. 1972. Hugoniot's method applied to stratified flow through a constriction. *J. Mech. Eng. Sci. 14*, 72–73.

Brogmus, W. 1952. Eine Revision des Wasserhaushaltes der Ostsee. *Kieler Meeres-forsch. 9*, No. 1.

Brush, L. M., Jr. 1970. Artificial mixing of stratified fluids formed by salt and heat in a laboratory reservoir. *Research Project B-024-New Jersey Water Resource Institute.*

Crapper, P. F. 1973. *An experimental study of mixing across density interfaces.* Ph.D. Dissertation, University of Cambridge.

Crapper, P. F. & Linden, P. F. 1974. The structure of turbulent density interfaces. *J. Fluid Mech. 65*, 45–63.

Cromwell, T. 1960. Pycnoclines created by mixing in an Aquarium tank. *J. Mar. Res. 18*, 73–82.

Fonselius, S. H. 1962. Hydrography of the Baltic deep basins. *Fishery Bd. of Sweden*, Series Hydrography, No. 13, 41 pp.

Fonselius, S. H. 1967. Hydrography of the Baltic deep basins II. *Fishery Bd. of Sweden*, Series Hydrography, No. 20, 31 pp.

Fonselius, S. H. 1969. Hydrography of the Baltic deep basins III. *Fishery Bd. of Sweden*, Series Hydrography, No. 23, 97 pp.

Gade, H. 1970. *Hydrographic investigations in the Oslofjord. A study of water circulations and exchange processes*, Vols I, II and III. Geophys. Inst. Univ. of Bergen, Norway.

Kato, H. & Phillips, O. M. 1969. On the penetration of a turbulent layer into a stratified fluid. *J. Fluid Mech. 37*, 643–655.

Kullenberg, B. 1955. Restriction of the underflow in a transition. *Tellus 7*, 215–217.

Linden, P. F. 1973. The interaction of a vortex ring

with a sharp density interface: a model of turbulent entrainment. *J. Fluid Mech. 60*, 467–480.
Long, R. R. 1973. Some properties of horizontally homogeneous, statistically steady turbulence in a stratified fluid. *Bdy.-Layer Meteor. 5*, 139–147.
Long, R. R. 1975*a*. Circulations and density distributions in a deep, strongly stratified, two-layer estuary. (To be published in *J. Fluid Mech.*)
Long, R. R. 1975*b*. The influence of shear on mixing across density interfaces. (To be published in *J. Fluid Mech.*)
Moore, M. J. & Long, R. R. 1971. An experimental investigation of turbulent stratified shearing flow. *J. Fluid Mech. 49*, 635–655.
Pickard, G. L. & Rodgers, K. 1959. Current measurements in Knight Inlet, British Columbia. *Fish. Res. Bd. Canada 16*, 635–678.
Pritchard, D. W. 1956. The dynamic structure of a coastal plain estuary. *J. Mar. Res. 15*, 33–42.
Rouse, H. & Dodu, J. 1955. Turbulent diffusion across a density discontinuity. *La Houille Blanche 10*, 405–410.
Stommel, H. & Farmer, H. G. 1952. Abrupt change in width in two-layer open channel flow. *J. Mar. Res. 11*, 205–214.
Stommel, H. & Farmer, H. G. 1953. Control of salinity in an estuary by a transition. *J. Mar. Res. 12*, 13–20.
Tully, J. P. 1949. Oceanography and prediction of pulp mill pollution in Alberni Inlet. *Bull. Fisheries Res. Board Can. 83*, 1–169.
Turner, J. S. 1968. The influence of molecular diffusivity on turbulent entrainment across a density interface. *J. Fluid Mech. 33*, 639–656.
Turner, J. S. 1973. *Buoyancy effects in fluids*. Cambridge Univ. Press (see Chapter 9).
Welander, P. 1974. Two-layer exchange in an estuary basin with special reference to the Baltic Sea. *J. Phys. Oceanogr. 4*, 542–556.
Wolanski, E. 1972. *Turbulent entrainment across stable density-stratified liquids and suspensions*. Ph.D. Dissertation, The Johns Hopkins University.
Wu, J. 1973. Wind-induced turbulent entrainment across a stable density interface. *J. Fluid Mech. 61*, 275–287.

ПЕРЕНОС МАССЫ И СОЛИ И ГЛУБИНА ГАЛОКЛИНА В УСТЬЕ РЕК

В статье рассматриваются потоки солоноватой и океанской вод из устья и в него, а также глубина галоклина в устье. В обсуждении игнорируются детали распределения массе воды в устье (за исключением глубины галоклина), а внимание концентрируется на определении условий течения и глубины поверхности раздела вблизи устья. Течение рассматривается без трения, давление гидростатическим и в первой части анализа, где предположено сильное перемешивание (и, поэтому, глубокий галоклин), получены те же результаты, что у Стоммела и Фармера для их «сильно перемешанного» состояния. Явления в этом состоянии определяются безразмерным числом Q_f, пропорциональным притоку пресной воды q_f. С другой стороны задача также может быть решена, когда перемешивание равно нулю. Два предельных случая предполагают зависимость от числа смешения M и для случая произвольного перемешивания. Это позволяет получить полное решение, описывающее поток океанской воды, поток солоноватой воды, глубину поверхности раздела в устье, соленость солоноватой воды, глубину галоклина в основной массе вады в устье и высоту свободной поверхности над уровнем моря в устье — все в виде функций от Q_f и M. Интересной особенностью всех решений является глубина главного галоклина, которая оказывается большой как для слабого, так и сильного притоков свежей воды и поэтому она имеет минимум при некоторой величине q_{fm}, меняющейся с M. Такое поведение наблюдалось во фьорде Алберни в Британской Колумбии и в лабораторном эксперименте Веландера. Применение теории к Балтийскому морю ведет к некоторым численным результатам и спекуляциям.